Analysis and Optimization of Fibre-Metal Laminate Cylindrical Shells Subjected to Transverse Impact Loads

R. Azarafza*, A. Davar

Faculty of Materials & Manufacturing Technologies, Malek Ashtar University of Technology, Iran

ABSTRACT: The main aim of the present paper is multi-objective optimization of circular cylindrical shells composed of fibre metal laminate. For this purpose, the genetic algorithms method is applied for optimization of combination of the objective functions including weight and transverse impact response and two constraints including critical buckling loads and principle strains. The initial compressive stress is taken to be equal to half of the axial critical buckling load of the shell. Nine design variables including material properties (fibre and matrix), volume fraction of fibre, fibre orientation, and volume fraction of metal layers are considered. In analytical solution, transient dynamic response due to low-velocity transverse impact of a large mass on the mid-span of composite circular cylindrical shells is investigated based on the first-order shear deformation shell theory and mode superposition method. The impact force of an isotropic sphere impactor is calculated using a Two-Degree-Of-Freedom (TDOF) spring-mass model. Different fibre metal laminate layups are considered for optimization and the results are compared. Results show that fibre metal laminate layup with 2/1 configuration has the smallest weight and impact response as compared to the other layups.

1. INTRODUCTION

Fiber-metal Laminate (FML) is a hybrid composite material combining thin metal layers with adhesive fibre prepreg as shown in Fig. 1.

They combine good characteristics of metals such as ductility, impact, and damage tolerances with the benefits of fibre composite materials such as high specific strength, high specific stiffness, and good corrosion and fatigue resistance. The Metal Volume Fraction (MVF) is defined as the sum of the ratio of thicknesses of the individual aluminum layers to the total thickness of the laminate [2]:

$$MVF = \sum_{1}^{p} h_{al} / h \qquad (1)$$

where h_{al} is the thickness of each separate aluminum layer and p is the number of aluminum layers and h is the total thickness of the laminate. Hence, $MVF=0$ and $MVF=1$ represent pure composite and pure metal shells, respectively. Due to the above advantages, cylindrical shells composed of FML materials are favorable to be used in advanced industries such as automobile, aircraft, and aerospace. Most FML cylindrical shells are subjected to impact loads and application
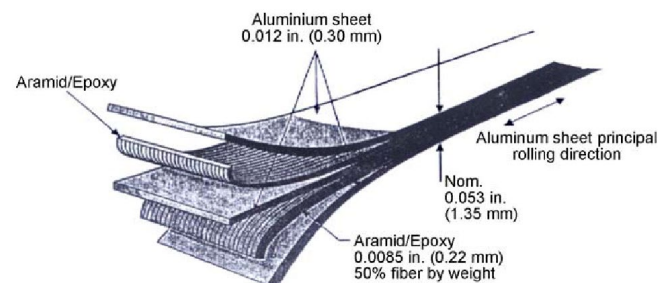

Fig. 1. Stacking sequence of the cross-section of the FML shell [1]

of this loading may cause an undesired deformation and strength reduction. Therefore, considering the impact response of these structural components is necessary for the design process. The orthotropic material properties of FMLs cause the need for optimization in the process of design and manufacturing of these hybrid constructions. The design variables in the optimization process are fibre orientation, material properties, volume fraction of fibre in prepreg layers, and MVF. Since the design process for the FMLs consist of many local minimum and maximum points and these points are not well distributed, therefore there is a need for a method to recognize these local and global optimum points and hence to find the global optimization [3]. Optimization with Genetic

*Corresponding author's email: azarkntu@yahoo.com

Algorithms (GA) is offered for such problems and has gained substantial attention in recent years. This technique is well known for robustness and ability to search complex and noisy search space, phenomena that are frequently encountered in designing and optimization problems especially for hybrid composite materials such as FMLs GA is a probabilistic global optimization method, in which the design variables are coded into individual genes or chromosomes and for which an individual design has one or more chromosomes. This optimization method works with a population of design rather than a single design. New generations of design evolve from previous generations by applying crossover and mutation operations to the genetic string in a manner similar to the evolution process of living creatures. Moreover, an individual design that has high fitness has also a probability of producing descendants. Many types of research have been done on the buckling, free vibration, and dynamic response of composite cylindrical shells. Geier et al.[4] studied the effect of stacking sequence on the buckling of the simply-supported cylindrical shell under axially compressive loads. Ng et al. [5] presented the dynamic stability analysis of cylindrical panels taking into account the transverse shear effects. Li and Chen [6] investigated transient dynamic response analysis of orthotropic circular cylindrical shells subjected to external hydrostatic pressure. They used classical shell theory and considered simply-supported boundary conditions. Lam and Loy [7] studied the influence of boundary conditions for a thin laminated rotating cylindrical shell using first Love's approximation and Galerkin method. Lee and Lee [8] studied the free vibration and dynamic response for the cross-ply composite circular cylindrical shell under radial impulse load and the boundary conditions were considered to be simply supported. Matemilola and Stronge [9] developed an analytical solution for the impact response of a simply-supported anisotropic composite cylinder. Sheinman and Greif [10] developed a general analytical and numerical method used for free and forced vibration of thin shells of revolution made of multi-layered elastic orthotropic materials with arbitrary stacking sequence. Khalili et al. [11] studied the free and forced vibration of simply supported composite circular cylindrical shells. The dynamic response was studied under transverse impulse, axial load, and internal pressure by modal technique. However, according to the best knowledge of the authors, the impact response of FML cylindrical shells has not been reported. In the analysis of the impact on cylindrical shells, commonly two parameters are of major concern. The first parameter is the estimation of contact force and the second one is the prediction of displacements as well as strains in the target structure due to the impact. Most of the researchers used Hertizan contact law or its modified version for the proper estimation of contact force between the impactor and the target during the impact event [12]. In the open literature, some researchers dealt with the optimization of composite structures. Riche and Haftka [13] used GA for optimization of laminate stacking sequence for buckling load maximization. Smerdov [14] carried out a computational study for optimum formulations of optimization problems on laminated cylindrical shells for buckling under external pressure. It was indicated that increasing the number of layers (more than four) does not result in increasing the buckling load. Weaver [15] used a computational study for designing the laminated composite cylindrical shells under axial compression to minimize the mass with local and global constraints. Duvaut et al. [16] developed a finite element discretization for determining the optimal direction and the volume fraction of fibre at each point of a structure to minimize the weight and the cost. Hu and Ou [17] used a sequential linear programming method with a simple move-limit strategy for maximization of the fundamental frequency of laminated truncated conical shells with respect to the fibre orientations. Park et al. [18] used GA for optimization of laminate stacking sequence to maximize the strength. Adali and Verijenko [19] optimized the stacking sequence design for hybrid laminates under free vibration to minimize the design cost. Soremekun et al. [20] used GA for stacking sequence blending of multiple composite laminates to minimize the weight and the cost of the panels and presented a methodology for designing the two-dimensional array of laminated composite panels with varying loads. Jaszkiewicz [21] studied a new genetic local search for multi objective combinatorial optimization and indicated that the GA is a good method for multi objective functions. Azarafza et al. [22] studied analysis and optimization of laminated composite circular cylindrical shell subjected to compressive axial and transverse transient dynamic loads. Their results show that the weight coefficient of multi-objective function and the type of the constraints have a considerable effect on the optimum weight and dynamic response. Taskin et al. [23] used the Generalized Differential Quadrature Method (GDQM) for the natural frequencies and loss factors of composite sandwich shells with frequency-dependent viscoelastic core. Rezvani et al. [24] investigated the dynamic response of the structures in the vicinity of railway tracks. The methodology of solution included the assumption of the elastic half space for the transfer medium. Arikoglu [25] studied the multi-objective optimal design of hybrid viscoelastic/composite sandwich beams for minimum weight and minimum vibration response is aimed. The equation of motion for linear vibrations of a multi-layer beam is derived by using the principle of virtual work in the most general form. Pang et al. [26] used the Jacobi-Ritz method for free and forced vibration analysis of airtight cylindrical vessels consisting of elliptical, paraboloidal, and cylindrical shells. Flügge's thin shell theory was adopted for the calculation model of vessels. Dinh and Nguyen [27] studied the linear dynamic response and vibration of Functionally Graded (FG) carbon nanotube-reinforced composite truncated conical shells resting on elastic foundations based on the classical shell theory. Tooti et al. [28] studied the free vibration of a functionally graded cylindrical shell made up of stainless steel, zirconia, and nickel. The equations of motion are derived by Hamilton's principle. Galerkin method is used to derive the governing equations.

According, no research has been observed by the authors in the literature on the optimization of the

dynamic response of FML cylindrical shells. Hence, the objective of this study is to optimize the weight and the impact response of FML circular cylindrical shell subjected to two constraints (critical buckling load and allowable strains) and with nine design variables. Multi-objective formulation is carried out by applying a weight coefficient to weight and impact response. For this purpose, first, the equilibrium equations of linear (eigenvalue) buckling and free vibrations for the shell are solved using the Galerkin method to obtain critical axial buckling load and natural frequencies subjected to the initial compressive stress equal to half of the axial critical buckling load of the shell. Second, the analysis of quasi-static low-velocity impact response of simply-supported FML circular cylindrical shells due to striking of a large mass steel sphere, based on first-order shear deformation theory, the displacement components are taken to be the product of a function of position and a function of time. The ratio of the mass of the impactor to the total mass of the FML cylindrical shell is assumed to be large enough so that the impact response could be categorized as quasi-static impact. Accordingly, a two-degree-of-freedom spring-mass model is applied or calculation of the contact force history. The contact force is distributed over a small square area. The impact point can be everywhere on the shell, but here it is assumed to be at the mid-span of the shell. But, the velocity of the impactor is low so that large deformation does not occur. The function of time is obtained using the results of free vibrations and convolution integrals. The time response of displacement components is derived using the mode superposition method. Third, the optimization of nine FML design parameters for weight and impact response minimization is investigated using GA. The influence of varying optimization parameters on the convergence of the solutions is investigated. Furthermore, the effects of some FML parameters such as MVF and FML layup on the impact response of the shells are investigated. The new interesting results are presented which provide helpful insight for aircraft fuselage skin designers. A laminate coding system is used to comprehensively define FML laminates. The code for glass-reinforced aluminum laminate is Al/G (1+i)/i [0/90]$_s$, for example, for i=4, Al/G 5/4 [0/90]$_s$, defined a laminate composed of five aluminum layers and four glass-reinforced polymer perpregs with lay up [0/90]$_s$ alternatively stacked together. The thicknesses of all aluminum layers are assumed to be the same. Also, the thicknesses of all composite layers are assumed to be the same.

2. GOVERNING EQUATIONS

A circular cylindrical shell with the mean radius of R, the thickness h, and the length L is shown in Fig. 2.

u, v, and w are the displacement components in the axial, tangential, and radial directions, respectively, and the deformations are assumed to be small. Based on first-order shear deformation theory, the equilibrium equations for a cylindrical shell are as follows [8, 22, 29, 30]:
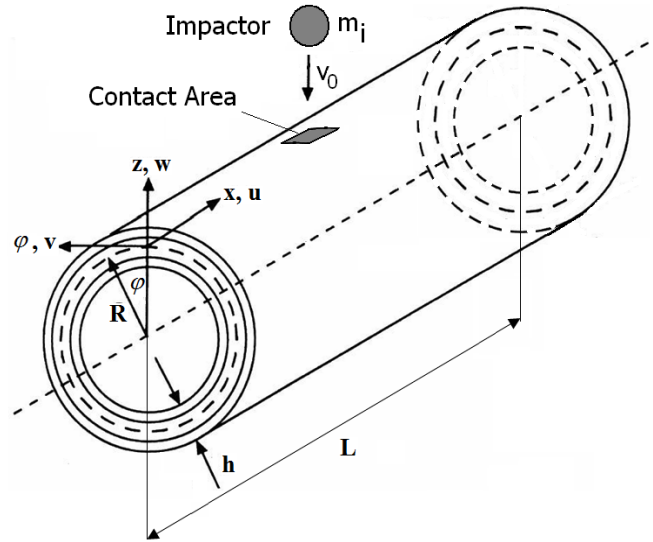

Fig. 2. Geometry and coordinate system of the cylindrical shell subjected to the transverse impact of a steel sphere

$$\frac{\partial N_x}{\partial x} + \frac{\partial N_{x\varphi}}{R\partial \varphi} + q_x(x,\varphi,t) = I_1 \frac{\partial^2 u}{\partial t^2} + I_2 \frac{\partial^2 \beta_x}{\partial t^2}$$

$$\frac{\partial N_{x\phi}}{\partial x} + \frac{\partial N_\phi}{R\partial \phi} + \frac{Q_\phi}{R} + N_a \frac{\partial^2 v}{\partial x^2} + q_\phi(x,\phi,t) =$$

$$(I_1 + \frac{2I_2}{R})\frac{\partial^2 v}{\partial t^2} + (I_2 + \frac{I_3}{R})\frac{\partial^2 \beta_\phi}{\partial t^2} \qquad (2)$$

$$\frac{\partial Q_x}{\partial x} + \frac{\partial Q_\varphi}{R\partial \varphi} - \frac{N_\varphi}{R} + N_a \frac{\partial^2 w}{\partial x^2} + q_r(x,\varphi,t) = I_1 \frac{\partial^2 w}{\partial t^2}$$

$$\frac{\partial M_x}{\partial x} + \frac{\partial M_{x\varphi}}{R\partial \varphi} - Q_x + m_x(x,\varphi,t) = I_3 \frac{\partial^2 \beta_x}{\partial t^2} + I_2 \frac{\partial^2 u}{\partial t^2}$$

$$\frac{\partial M_{x\varphi}}{\partial x} + \frac{\partial M_\varphi}{R\partial \varphi} - Q_\varphi + m_\varphi(x,\varphi,t) = I_3 \frac{\partial^2 \beta_\varphi}{\partial t^2} + (I_2 + \frac{I_3}{R})\frac{\partial^2 v}{\partial t^2}$$

In the above equations, β_x and β_φ are the slopes in planes of x-z and $\varphi - z$, respectively. Also, q_x, q_φ and q_r are the external forces, m_x and m_φ are the external moments that excite the shell. N_a is the axial load. I_1, I_2 and I_3 are mass moments of inertia. Also, N, M, and Q are stress resultants [8, [30]. All deformations are assumed to be small according to Love's first-approximation theory. Accordingly, the maximum defection under impact point must be linear, i.e. it must be less than or almost equal to the FML shell wall thickness. All of the equivalent material properties for each prepreg layer are obtained using the rule of mixture which is well defined by Tsai [31].

3. BOUNDARY CONDITIONS

The boundary conditions for the cylindrical shell which is simply supported along its curved edges are considered as [8]:

$$N_x(0,\phi,t) = N_x(L,\phi,t) = 0,$$
$$M_x(0,\phi,t) = M_x(L,\phi,t) = 0 \tag{3}$$
$$w(0,\phi,t) = w(L,\phi,t) = 0,$$
$$v(0,\phi,t) = v(L,\phi,t) = 0$$

In order to solve the free vibration problem, the external excitations are taken to be zero. After substituting stress resultant relations [830] into the Eq. (2), the results are simplified in the following form:

$$[L]\{U\} = \{0\} \tag{4}$$

where

$$L = \begin{bmatrix} L_{11} & L_{12} & L_{13} & L_{14} & L_{15} \\ L_{21} & L_{22} & L_{23} & L_{24} & L_{25} \\ L_{31} & L_{32} & L_{33} & L_{34} & L_{35} \\ L_{41} & L_{42} & L_{43} & L_{44} & L_{45} \\ L_{51} & L_{52} & L_{53} & L_{54} & L_{55} \end{bmatrix}, \{U\} = \begin{Bmatrix} u(x,\varphi,t) \\ v(x,\varphi,t) \\ w(x,\varphi,t) \\ \beta_x(x,\varphi,t) \\ \beta_\varphi(x,\varphi,t) \end{Bmatrix} \tag{5}$$

L_{ij} are the anti-symmetric differential operators and are well defined by Jafari *et al.* [30].

To satisfy the boundary conditions, u, v, w, β_x and β_φ are defined by the following double Fourier series [7,8]:

$$u = \sum_m \sum_n \overline{A}_{mn} T_{mn}(t) = \sum_m \sum_n A_{mn} \cos\frac{m\pi x}{L} \cos n\varphi T_{mn}(t)$$

$$v = \sum_m \sum_n \overline{B}_{mn} T_{mn}(t) = \sum_m \sum_n B_{mn} \sin\frac{m\pi x}{L} \sin n\varphi T_{mn}(t) \tag{6}$$

$$w = \sum_m \sum_n \overline{C}_{mn} T_{mn}(t) = \sum_m \sum_n C_{mn} \sin\frac{m\pi x}{L} \cos n\varphi T_{mn}(t)$$

$$\beta_x = \sum_m \sum_n \overline{D}_{mn} T_{mn}(t) = \sum_m \sum_n D_{mn} \cos\frac{m\pi x}{L} \cos n\varphi T_{mn}(t)$$

$$\beta_\varphi = \sum_m \sum_n \overline{E}_{mn} T_{mn}(t) = \sum_m \sum_n E_{mn} \sin\frac{m\pi x}{L} \sin n\varphi T_{mn}(t)$$

In the above equations, $T_{mn}(t)$ is the function of time. Also, A_{mn}, B_{mn}, C_{mn}, D_{mn} and E_{mn} are the constant coefficients of the natural mode shapes associated with the free vibration problems, m is the axial half-wave and n is the circumferential wave number. Galerkin method is used to solve the differential equations in Eq. (4).

4. METHOD OF ANALYSIS
4.1 Linear buckling analysis

In the linear buckling analysis, it is assumed that the material and the geometry of the shell are perfect and no imperfection exists. For calculating the static buckling load, the static solution is performed. Solving Eq. (4) by Galerkin method and after simplification, the following equation is obtained:

$$[C_{ij}]\{A_{mn}\ B_{mn}\ C_{mn}\ D_{mn}\ E_{mn}\}^T = [[K_{ij}] - [\overline{N}]]$$
$$\{A_{mn}\ B_{mn}\ C_{mn}\ D_{mn}\ E_{mn}\}^T = 0 \qquad (i,j=1,...,5) \tag{7}$$

K_{ij} is stiffness matrix and $\overline{N}$ is load matrix whose elements are given in Appendix. By setting determinant of the coefficients equal to zero, the buckling loads equation is derived as:

$$\gamma_1 N_{cr}^2 + \gamma_2 N_{cr} + \gamma_3 = 0 \tag{8}$$

where γ_i are the constant coefficients and N_{cr} is the axial critical buckling load.

4.2 Free vibration analysis

To solve the free vibration analysis, the function of time is treated as $T_{mn}(t) = e^{i\omega_{mn}t}$ where ω_{mn} is the natural frequency. By applying a method similar to the buckling analysis, the following set of equations can be derived:

$$[[K_{ij}] - \omega_{mn}^2[M_{ij}]]\{A_{mn}\ B_{mn}\ C_{mn}\ D_{mn}\ E_{mn}\}^T = 0$$
$$(i,j=1,...,5) \tag{9}$$

where K_{ij} and M_{ij} are the stiffness and mass matrices whose elements are given in Appendix. By setting the determinant of the coefficients equal to zero, the characteristic frequency equation is derived as:

$$\delta_1\omega^{10} + \delta_2\omega^8 + \delta_3\omega^6 + \delta_4\omega^4 + \delta_5\omega^2 + \delta_6 = 0 \tag{10}$$

where δ_i are the constant coefficients. By solving Eq. (10), natural frequencies are calculated, and by substituting these frequencies in Eq. (9), the constant coefficients of the mode shapes are obtained.

4.3 Dynamic response analysis

The load is assumed to be applied only in the radial direction. Hence:

$$\begin{cases} q_x(x,\phi,t) = q_\phi(x,\phi,t) = \\ m_x(x,\phi,t) = m_\phi(x,\phi,t) = 0 \\ q_r(x,\phi,t) = Q_r(x,\phi)f(t) = \\ [\sum_{m=1}^{\infty}\sum_{n=0}^{\infty} P_{mn} \sin\frac{m\pi x}{L} \cos n\phi]f(t) \end{cases} \tag{11}$$

The impact load is applied as a uniform pressure to a small square area located at the center point of the shell. Then the constant Fourier coefficients P_{mn} in Eq. (11) are:

$$n > 0, \qquad P_{m0} = \frac{-2}{m\pi^2}[\cos(\frac{m\pi x_2}{L}) -$$
$$\cos(\frac{m\pi x_1}{L})](\psi_2 - \psi_1)$$
$$n > 0, \qquad P_{mn} = \frac{-2}{mn\pi^2}[\cos(\frac{m\pi x_2}{L}) - \tag{12}$$
$$\cos(\frac{m\pi x_1}{L})][\sin(n\psi_2) - \sin(n\psi_1)]$$

After substituting Eq. (11) into the governing Eq. (2) and simplification, the generalized coordinate in Eq. (6) is obtained in the following form:

$$T_{mn}(t) = \frac{P_{mn}C_{mn}}{J_{mn}\omega_{mn}} \int_0^t f(\tau)\sin\omega_{mn}(t-\tau)d\tau \qquad (13)$$

Therefore, based on mode superposition theory, the time response of the cylindrical shell in the radial direction is:

$$w = \sum_m \sum_n \frac{P_{mn}C_{mn}^2}{J_{mn}\omega_{mn}} \sin\frac{m\pi x}{L}$$

$$\cos n\phi \int_0^t f(\tau)\sin\omega_{mn}(t-\tau)d\tau \qquad (14)$$

A brief description of the time response analysis is presented in this paper. More details could be found in the authors' earlier works [11,30].

4.4 Contact force history estimation

Configuration of the impact between the impactor and the cylindrical shell is shown in Fig. 2. A TDOF Spring-Mass (S-M) model for estimation of contact force history is presented herein. Assumptions, configuration, and parameters of the present model are described in the following sections.

4.4.1 Model assumptions

To calculate the contact force, the following assumptions are made:
- The impactor strikes with low-velocity and normal to the shell's outer surface.
- The shape of the impactor is spherical, with elastic isotropic material properties.
- Effects of strain rate and wave propagation on the impact response are neglected.
- The parts of the impactor's initial energy dissipated due to vibrations of the impactor body, thermal effects, acoustic emission, and local damage are neglected.

Since in the present analysis the effect of wave propagation due to impact is neglected, the problem of impact considered here is classified as boundary controlled impact, according to Olsson's classification [32]. Therefore, the impact behavior is assumed to be quasi-static in nature. Hence, long-time impact [32] due to the impact of a large mass is considered and discussed here.

4.4.2 TDOF Spring-Mass model

In Fig. 4, the present linear TDOF S-M model is shown. k_c^* and k_{bs} are effective contact and effective combined bending-shear stiffnesses, respectively, m_i and m_s^* are impactor mass and effective mass of the target structure, respectively.

It is assumed that the impactor strikes the shell with low-velocity v_0. Assuming other initial conditions to be zero and according to Newton's second law, equations of motion of the TDOF S-M model illustrated in Fig. 4, are stated as:

$$\begin{bmatrix} m_i & 0 \\ 0 & m_s^* \end{bmatrix}\begin{Bmatrix} \ddot{x}_i \\ \ddot{x}_s \end{Bmatrix} + \begin{bmatrix} k_c^* & -k_c^* \\ -k_c^* & (k_c^* + k_b) \end{bmatrix}\begin{Bmatrix} x_i \\ x_s \end{Bmatrix} = \begin{Bmatrix} 0 \\ 0 \end{Bmatrix} \qquad (15)$$

where x_i and x_s are system degrees of freedom (DOF). Similar formulation is used by Gong [12] and Shivakumar et al. [33]. The solution to this set of linear ordinary differential equations is reported by Gong [12]. The effective contact stiffness (k_c^*) used by Gong [12] is employed in the present TDOF S-M model. But, in the present TDOF S-M model, the effective mass (m_s^*) and effective static stiffness (k_{bs}) at the impact point of FML circular cylindrical shell are calculated and used based on the method reported by Swanson [34]. These parameters are determined in the following sections.

4.4.3 Determination of the contact force function

The contact force function $F_c(t)$ is determined as:

$$F_c(t) = k_{bs}x_s(t) = \frac{k_{bs}v_0(k_c^* - m_i\omega_2^2)(k_c^* - m_i\omega_1^2)}{k_c^* m_i(\omega_2^2 - \omega_1^2)}$$

$$\left(\frac{\sin(\omega_1 t)}{\omega_1} - \frac{\sin(\omega_2 t)}{\omega_2}\right) \qquad (16)$$

\where ω_1 and ω_2 are the natural frequencies of the TDOF S-M system. The time function $f(t)$ of the external excitation $q_z(x,\varphi,t)$ in Eq. (11) is determined by dividing the contact force function in Eq. (16) to the contact area which is considered to be a small square patch of area A_L as follows [35]:

$$\begin{cases} f(t) = \dfrac{F_c(t)}{A_L} = F_0\left(\dfrac{\sin(\omega_1 t)}{\omega_1} - \dfrac{\sin(\omega_2 t)}{\omega_2}\right), & 0 \le t \le T \\ f(t) = 0, & t > T \end{cases} \qquad (17)$$
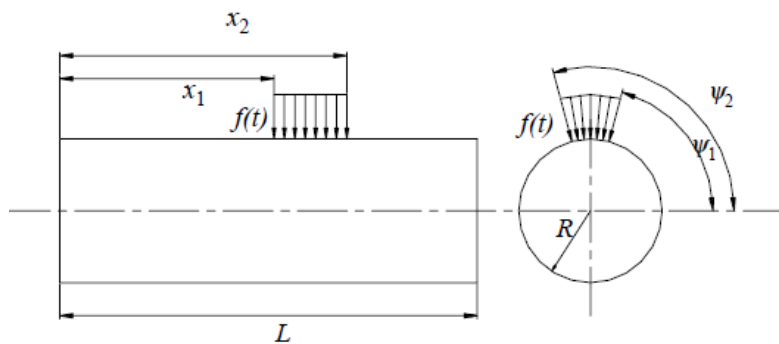

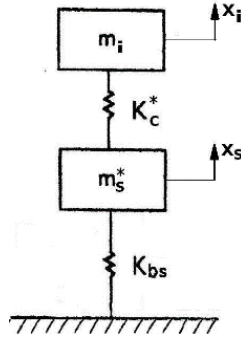**Fig. 3. Geometric parameters defining the size and position of the area of the applied load**

Fig. 4. Linear TDOF S-M model used in the present study

$$F_0 = \frac{k_{bs} v_0 (k_c^* - m_i \omega_2^2)(k_c^* - m_i \omega_1^2)}{A_L k_c^* m_i (\omega_2^2 - \omega_1^2)} \qquad (18)$$

where in Eq. (17), T is Contact Time (CT). Then, substituting Eq. (17) into Eq. (14), the time history of the radial displacement of the shell at the contact point is calculated.

5. OPTIMIZATION

The design variables for an FML circular cylindrical shell are FML design parameters including Metal Volume Fraction (MVF), material properties of fiber and matrix, fiber orientations, and volume fractions of fiber in prepreg layers. These are continuous design variables and are taken from their specified intervals. Hence, the gradient-based optimization methods are not suitable for the optimal design of FML circular cylindrical shells. Furthermore, owing to manufacturing constraints, a family of good optimum designs is needed rather than a single point design. GA is a method for evolving a given design problem to a family of near-optimum designs [13]. Stochastic processes are used to generate an initial population of individual design and the process then applies the principle of natural selection and survival of the fittest to find improved design. Furthermore, since the discrete design procedure works with a population of designs, it can explore large design space and climb different hills. This is a major advantage as the converged solution may contain many optimal of comparable performance. The population or family of good design produced by GA may include the global optimum design, rather than a single design. Hence, it is an appropriate tool for designing general FML circular cylindrical shell.

6. DESIGN PROBLEM DEFINITION

The present design problem is to minimize the weight and to improve the impact response of the FML circular cylindrical shell for a given design loading condition. The design sought here is a cylinder of minimum weight and improve impact response in certain design space with static axial and lateral impact load, but not buckled or failed due to the excessive strain. Design variables are MVF, Young's modules (E_{fi}, E_{mi}), Poisson's ratios (v_{fi}, v_{mi}), densities (ρ_{fi}, ρ_{mi}), volume fraction of fibre (V_{fi}), fibre orientation (θ_i). Subscripts f

and m represent fibre and matrix, respectively, and subscript i represents the ith layer. It is to be noted that the overall material properties of each layer are calculated from the well-known rule of mixture [31].

This design problem can be defined by setting up the optimization procedures in the following way. The input data are the length, the mean radius, the axial compressive load (N_a), the allowable strains in principal directions (ε_{11}^{all}, ε_{22}^{all} and γ_{12}^{all}) for metal and prepreg layers, the mass, velocity, and radius of the spherical impactor, the position of the applied load (mid-span of the shell), the required mode numbers ($m \times n$) for sufficient convergence, the weight coefficient (α) and the probabilities of mutation (P_m) and crossover (P_c). Also, the bounding values of design variables are input to the analysis. The formulation of multi-objective optimization is carried out. The weight of FML shell (W) which has N layers ($N = N_m + N_p$ where N_m is the total number of metal layers and N_p is the total number of each prepreg layers.) is equal to:

$$W = gL\pi \left[\sum_{i=1}^{N_p} (r_{i+1}^2 - r_i^2)(\rho_{fi}V_{fi} + \rho_{mi}V_{mi}) + \sum_{i=1}^{N_m} (r_{i+1}^2 - r_i^2)\rho_{al} \right] \qquad (19)$$

where g is the gravity acceleration, r_i and r_{i+1} are the inner and the outer radius of the ith layer, respectively and $V_{mi} = 1 - V_{fi}$. The objective functions are to minimize the weight (W) and to improve the impact response amplitude (w) of the shell which are formulated as a function of the design variables as follows:

$$W = f_1(\rho_{fi}, \rho_{mi}, V_{fi}, MVF); \qquad i = 1,2,...,N_p \qquad (20)$$

$$w = f_2(\rho_{fi}, \rho_{mi}, V_{fi}, E_{fi}, E_{mi}, v_{fi}, v_{mi}, \theta_i, MVF); \\ i = 1,2,...,N_p \qquad (21)$$

Constraints are critical buckling load and principle strains which are given as follows:

$$N_{cr} = f_3(V_{fi}, E_{fi}, E_{mi}, v_{fi}, v_{mi}, \theta_i, MVF); \\ i = 1,2,...,N_p \qquad (22)$$

The critical buckling load (N_{cr}) constraint must be greater than or equal to the preset axial compressive load (N_a), i.e. $N_{cr} \geq N_a$. Also, the in-plane principle strains as given in Eq. (23) must be less than or equal to the allowable strain constraints, i.e. $\varepsilon_{11} \leq \varepsilon_{11}^{all}$, $\varepsilon_{22} \leq \varepsilon_{22}^{all}$ and $\gamma_{12} \leq \gamma_{12}^{all}$ in both prepreg and metal layers:

$$\varepsilon_{11} = f_2(\rho_{fi}, \rho_{mi}, V_{fi}, E_{fi}, E_{mi}, v_{fi}, v_{mi}, \theta_i, MVF); \\ i = 1,2,...,N_p$$

$$\varepsilon_{22} = f_3(\rho_{fi}, \rho_{mi}, V_{fi}, E_{fi}, E_{mi}, v_{fi}, v_{mi}, \theta_i, MVF); \\ i = 1,2,...,N_p \qquad (23)$$

$$\gamma_{12} = f_4(\rho_{fi}, \rho_{mi}, V_{fi}, E_{fi}, E_{mi}, v_{fi}, v_{mi}, \theta_i, MVF); \\ i = 1,2,...,N_p$$

To satisfy the requirements of optimization, it is necessary to consider two coefficients: the coefficient for margin of safety for critical buckling load (λ_b) and the coefficient for margin of safety for principle ply strain (λ_s), that are:

$$\lambda_b = 1 - \frac{N_a}{N_c}, \qquad \lambda_s = 1 - \max\left\{\frac{\varepsilon_1}{\varepsilon_1^{all}}, \frac{\varepsilon_2}{\varepsilon_2^{all}}, \frac{\gamma_2}{\gamma_2^{all}}\right\} \tag{24}$$

To calculate the radial displacement response due to impact in Eqs. (21) and the in-plane principle strains in Eq. (23), the value N_a is taken to be zero. But, it is considered and assigned a particular value in Eq. (24) for comparing with N_{cr}.

7. MULTI-OBJECTIVE FUNCTION FORMULATION

The multi-objective optimization problem can be formulated concisely as:

$$MIN\ (W\ and\ w),\ \lambda_b > 0\ and/or\ \lambda_s > 0\quad Constriant \tag{25}$$

The multi-objective function formulation is carried out by using a convex combination of the weight objective function (ψ_W) and the impact response objective function (ψ_w). Since these two objective functions are not the same, then they should be non-dimensional.

$$\psi_W = \frac{W}{W_f}, \quad \psi_w = \frac{w}{w_f} \tag{26}$$

where W_f and w_f are the values of the weight and the impact response, respectively, regarding the bounding values primarily specified for the ranges of the design variables. Multi-objective function (Φ_M) is defined by the following relation:

$$\Phi_M = \alpha\psi_W + (1-\alpha)\psi_w\quad 0 \le \alpha \le 1 \tag{27}$$

where α is the weight coefficient. Considering buckling load and allowable strains constraints, the multi-objective function (Φ_M) takes the following form:

$$\Phi_M = \begin{cases} [\psi_W - \frac{\psi_W}{N}S]\alpha + [\psi_w - \frac{\psi_w}{N}S](1-\alpha) \\ \text{feasible laminates} \\ \\ [\psi_W(1-S)^P\alpha + \psi_w(1-S)^P(1-\alpha) \\ \text{infeasible laminates} \end{cases} \quad 0 \le \alpha \le 1 \tag{28}$$

where P is a constant which depends on violation of a constraint [36] and S is defined as:

$$S = \min\{\lambda_b, \lambda_s\} \tag{29}$$

In Eq. (27), $\alpha = 0$ represents impact response optimization only. Also $\alpha = 1$ represents weight optimization only. In this study, for multi-objective optimization, i.e. weight and impact dynamic response, the value α is set to a number between 0 and 1. Finally, the fitness function expression corresponded to multi-objective function (F_M) is defined as follows:

$$F_M = \frac{1}{\Phi_M} \tag{30}$$

As the weight and the impact response are to be minimized, then F_M should be maximized.

8. NUMERICAL RESULTS

Results are presented for FML circular cylindrical shell subjected to the axial compression and the lateral impact loads to minimize weight and impact response subjected to the constraints of critical buckling load and the allowable strains. Hereinafter, everywhere otherwise stated, the cylindrical shell with length L=1m and radius R=1m is considered. The considered thin-walled FML shell may be used as primary structural components such as load transmitting parts in aircraft structures and pressurized fuel tanks where applicable thickness-to-radius ratios (h/R) may vary from 0.002 up to 0.004, which is discussed in the following. To show the results clearly, some examples are presented. A computer program is written to optimize the design variables the maximized fitness (minimum weight and impact response) using GA. Input data used for the optimization process are as follows. The ranges of design variables are [22]:

$$\rho_{fi} = \{1380,...,7800\}\,\text{kg/m}^3,$$
$$E_{fi} = \{60, ...,483\}\,\text{GPa}, \quad v_{fi} = \{0.15,...,0.35\}$$

$$\rho_{mi} = \{1000,...,7800\}\,\text{kg/m}^3,$$
$$E_{mi} = \{0.7,...,5.5\}\,\text{GPa}, \quad v_{mi} = \{0.26,...,0.4\}$$

$$V_{fi} = \{0.5,...,0.7\},$$
$$\text{MVF} = \{0.0,...,0.70\}, \quad \theta_i = \{-90°,...,90°\}$$

W_f and w_f, the values of the weight and the impact response used in Eq. (26), regarding the bounding values of design variables, irrespective of the buckling and strain constraints are shown in Table 1.

In the case of strain constraint, allowable principle strains are set to be $\varepsilon_{11}^{all} = 9.89e\text{-}3$, $\varepsilon_{22}^{all} = 3.87e\text{-}3$ and $\gamma_{12}^{all} = 1.9e\text{-}3$ for prepreg layers [20] and $\varepsilon_{11}^{all} = 3.07e\text{-}3$, $\varepsilon_{22}^{all} = 3.07e\text{-}3$ and $\gamma_{12}^{all} = 4.08e\text{-}3$ for aluminum layers [38]. In the case of buckling constraint, the value of the axial compressive load, which is only used in Eq. (24) and to be compared with the critical buckling load of the shell (N_{cr}), is $N_a = 0.5N_{cr}$.

GA control parameters are population size (P.S. =50), probability of crossover (P_c =0.5), and the probability of mutation (P_m =0.003) with linear deterministic rule decrements. Although, the probability of mutation is usually less than 0.001, but the great value selection with linear deterministic decrements allows exploring and exploiting of searching space to find the optimum solution and prevent convergence to a local optimum. Three different values for weight coefficient (α) are utilized for multi-objective optimization in this study (i.e. $\alpha = 0.3$, $\alpha = 0.5$ and $\alpha = 0.7$). All of the genetic operations are repeated until obtaining a converged solution.

8.1. Verification of the analytical model for contact force estimation

The material properties related to Figs. 5 to 9 are shown in Table 2.

To verify the TDOF S-M impact model, the history of contact force for pure composite and FML cylindrical shells, are compared in Figs. 5 and 6, respectively.

As indicated in Fig. 5, the result of the present impact model has a good correlation with analytical and experimental results reported by Matemilola and Stronge [9] and Gong [12]. The discrepancy between the present results with the experimental result by Gong [12] for maximum contact force is less than -4.3% and the discrepancy contact time is less than 1.6%. Fig. 10.2 presents a comparison between the results of contact force history of the present impact model with those obtained using an FEM model made in ABAQUS explicit solver. In the FEM model, S4R element is used for modeling the cylindrical shell and R3D4 and R3D3 element are used for modeling the impactor. As can be seen from this figure, similar trends are observed. The discrepancy between the present results with ABAQUS/Explicit results for maximum contact force is less than 11.6% and the absolute discrepancy

for contact time is less than 8.2%. As it is shown in Figs. 5 and 6, the results are in good agreement.

8.2 Verification of the optimization procedure
8.2.1 Investigation of GA capability to find global optimum

To investigate the convergence of GA to the global optimum point, maximum radial displacement response surface versus fibre orientation (θ) and MVF as design variables for an Al/prepreg $5/4\,[\theta/-\theta]_2$ FML cylindrical shell is derived in Fig. 7.

As can be seen in Fig. 7, there are two local minimum points for $w_{\max}$. But as indicated in Fig. 8, GA escapes the local minimums and rapidly finds the global minimum.

Fig. 8 shows the progress in the evolution of the design variables, i.e. fibre orientation θ and MVF, in the design space over the contour plot of the level lines corresponded to the response surface plot in Fig. 7.

Fig. 9 shows the convergence of the maximum fitness (F_M) versus G.N. and after 31 generations, the optimum fibre orientation and MVF are obtained.

The results in Fig. 9 represent a good capability of the GA to escape the local optimums and to find the global optimum

Table 1. Values of the weight response (W_f) and the dynamic response (w_f) used in Eq. (25), with respect to the bounding values of design variables, irrespective of the buckling and strain constraints

Number of prepreg layers		N_p=1, 2,3		
FML layup	2/1	3/2	4/3	5/4
Objective Function — w_f (mm)	4.7099	5.0295	5.1700	5.2491
W_f (N)		744.96		

Table 2. Ply properties used in Figs. 5-9

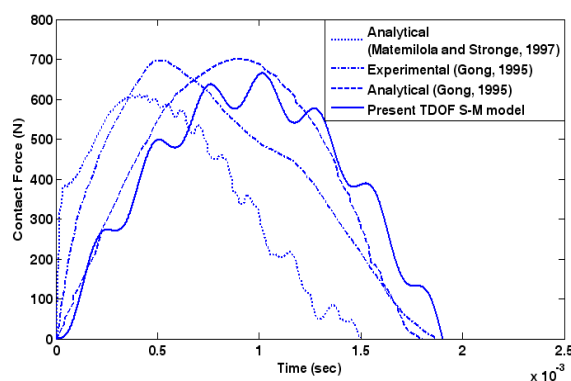| Fig. no.	Material	E_{11}[GPa]	E_{22}[GPa]	G_{12}[GPa]	G_{23}[GPa]	ν_{12}	ρ[kg/m^3]
Fig. 5	Glass/Epoxy (Gong, 1995)	14.506	5.362	2.509	2.509	0.231	1526
Figs. 6 to 9	Al 2024 T3 [37]	72.4	72.4	28.0	28.0	0.33	2770
	Glass/Epoxy [38]	60	13	3.4	3.4	0.3	2100

Fig. 5. Comparison of contact force histories due to impact of a steel sphere on a GRP cylinder
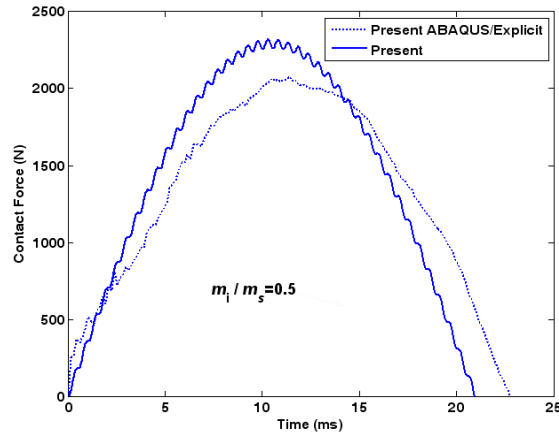
Fig. 6. Comparison of contact force histories due to impact of a solid sphere on an FML cylinder with layup Al/G 5/4 [0/90]s for the mass ratio of m_i/m_s=0.5
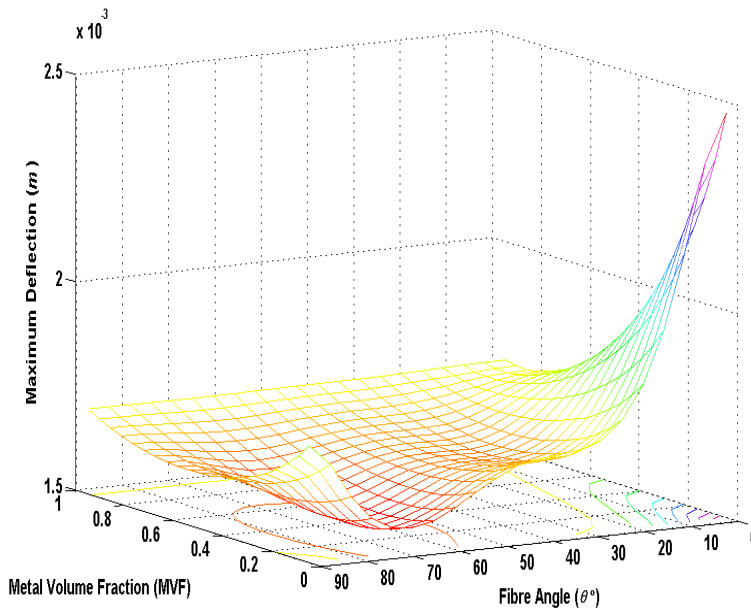

Fig. 7. Maximum radial displacement response surface variation versus the design variables, fibre orientations θ, and metal volume fraction (MVF), for an FML shell with the layup Al/Comp. 5/4 $[\theta/-\theta]_2$, to be compared with the results in the first column of Table 3 (No buckling and/or strain constraint).

rapidly. Table 3 shows the comparison between the results obtained by random search using GA, and these obtained by the complete (point by point) searching the design space. As can be seen in Table 3, the optimum values for fibre orientation (θ) and MVF obtained by GA are very close to those found through the present complete searching method.

8.2.2 Investigation of the convergence of the GA

Fig. 10 shows the convergence of fitness function (F_M) for Al/prepreg 2/1 FML cylindrical shells.

The results show that for small values of N_p, the minimum required G.N., as well as the run time for sufficient convergence, is lower rather than larger values of N_p, i.e. G.N. =79 is required for N_p =1, G.N. =97 for N_p =2 and G.N. =110 for

N_p =3. Fig. 11 shows the convergence of the fitness function for two population sizes i.e. P.S. =60 and P.S. =80.

In this figure, using P.S. =60, convergence is happened after about G.N. =110 and when P.S. =80, the convergence is happened after about G.N. =102, and the program run time for P.S. =80 is greater than that of P.S. =60. As the population is increased, the program run time is also increased and the number of generations in which convergence occurred is decreased. Fig. 12 shows two runs with the same input data for P.S. =60.

The minimum required G.N. at which the convergence occurred are G.N. =91 and G.N. =95 for the first and second runs, respectively. Hence, different runs converge approximately to the same value of fitness (i.e. $F_M \cong 6.8$ in
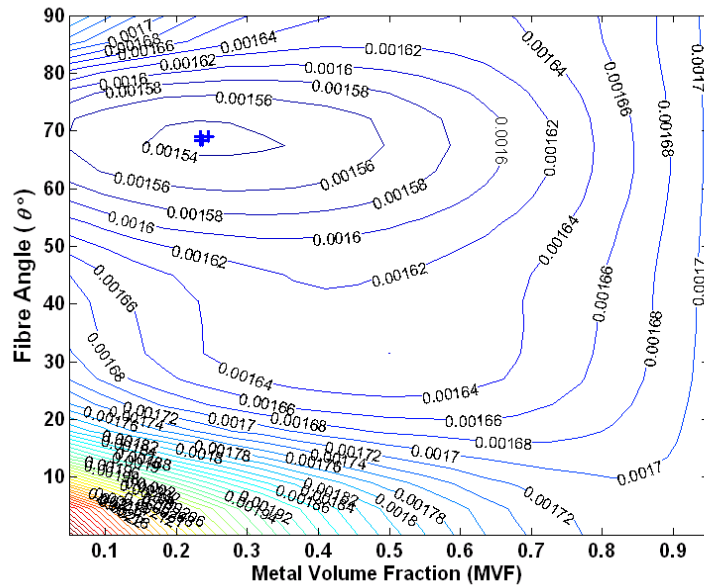
Fig. 8. Contour plot of level lines (lines with the same values on the response surface of the radial displacement response in Fig. 7) together with the progress in the evolution of the design variables θ_1 and θ_2 ;
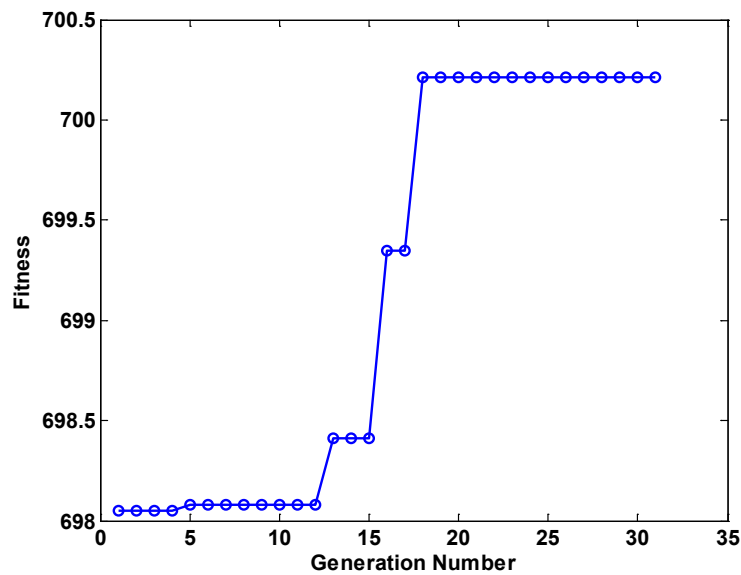

Fig. 9. Fitness (F_M) of the most fit chromosome versus G.N. for the generations shown in Fig. 7

Fig. 12). Figs. 13 to 16 show that the GA sweeps all the design space. Also, it can be seen in these figures that the selected design variables take different values between the upper and the lower limits preliminarily assigned to them. This point shows that all the design variables play an active role in the optimization process.

8.3 Discussion

In Table 4, different cases of the optimization parameters are classified. Different combinations of objective functions, constraints types, and weight coefficients are considered in

this table.

According to the cases defined in Table 4, in Table 5, the effects of optimization parameters including objective function, weight coefficient, and constraint type are investigated.

The effect of weight coefficient is studied by making a comparison between the optimization results of cases no. 1, 2, and 3 for "Response + Weight" as objective function and "Buckling + Strain" as constraint type defined in Table 4. The effect of constraint type is studied by making a comparison between the optimization results of cases no. 2, 4, and 5 for

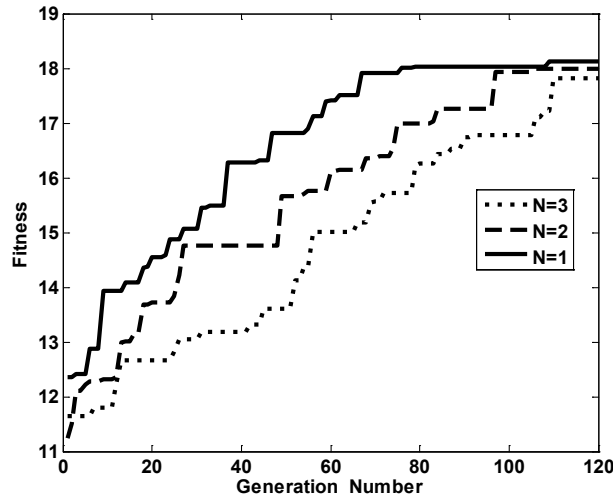|	Results obtained by GA	Results obtained by complete searching the design space
θ (deg)	68.5	68.1
MVF	0.23	0.225
w (m)	1.55e-3	1.54e-3

Fig. 10. Fitness (F_M) of the most fit chromosome versus G.N. for Al/prepreg 2/1 FML cylindrical shells ($\alpha = 0.5$, Constraints: buckling and strain).
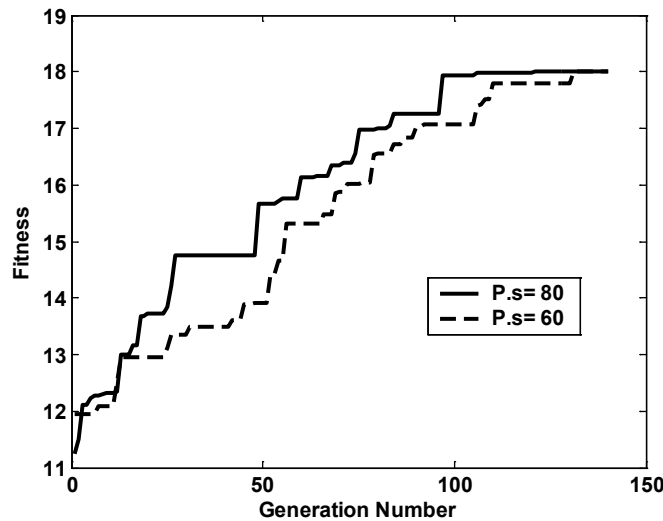

Fig. 11. Fitness (F_M) of the most fit chromosome versus *G.N.* for *P.S.*=60 and 80, for an Al/prepreg 2/1 FML cylindrical shell ($\alpha = 0.5$, Constraints: buckling and strain).

"Response + Weight" as objective function and cases no. 6, 7, and 8 for "Response" as an objective function, all with weight coefficient $\alpha = 0.5$ as defined in Table 4. The effect of the objective function is studied by making a comparison between the optimization results of cases no. 2 and 6 for "Buckling + Strain" constraint, cases no.4 and 7 for " Buckling " constraint, and cases no. 5 and 8 for " Strain " constraint, all with weight

coefficient $\alpha = 0.5$ as defined in Table 4. For each of cases no. 1 to 8 defined in Table 4, four layups including 2/1, 3/2, 4/3, and 5/4 are considered and the optimization process is done for a number of FML layups $N_p = 1,2,3$. Consequently, thirty-two (8×4) tables are produced according to Table 4. But, only case no. 4 in Table 4 is considered only and the corresponding results are presented in Tables 6 to 9 for layups 2/1, 3/2, 4/3,
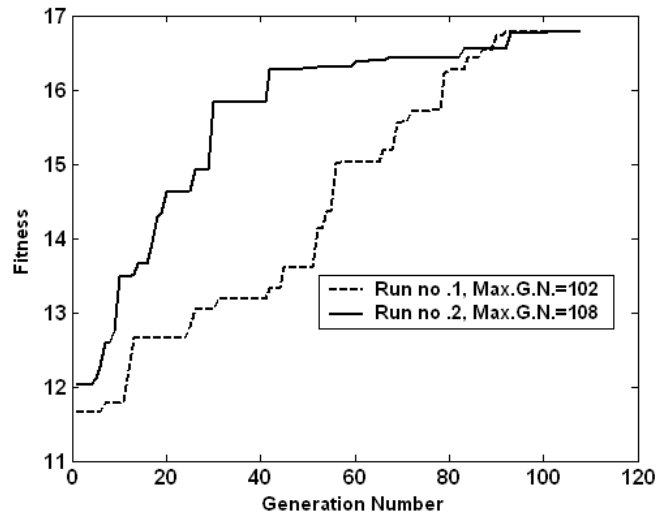
Fig. 12. Convergence of fitness value (F_M) for two different runs for a Al/prepreg 2/1 FML cylindrical shell. ($\alpha = 0.5$, Constraints: buckling and strain).
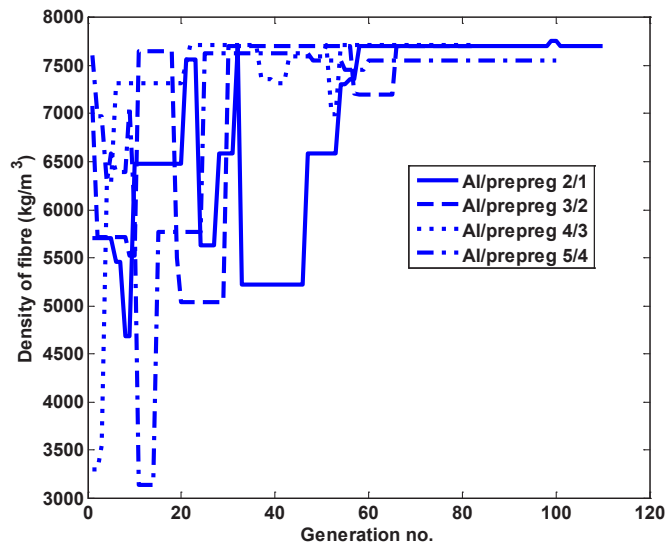

Fig. 13. Variation of ρ_{fi} versus *G.N.* for an Al/prepreg 2/1 FML cylindrical shell, (N_p=1).

and 5/4, respectively.

As it is clear in Tables 6 to 9, for a number of prepreg layers N_p greater than 1(>1), the smallest impact response is corresponded to lay up 2/1 (or Al/prepreg 2/1). Also, the smallest weight corresponds to a number of prepreg layers greater than 1 (N_p >1). For all the cases considered in these tables, the smallest weight corresponds to N_p =2. The greatest buckling load happens at N_p =2 for layup 2/1 and the smallest buckling load occurs at N_p =1 for layup 2/1. Hence, lay up 2/1 has more benefits as compared to the other layups. For the maximum strength ratio, no special trend could be observed.

For the sake of space-saving, the remaining 28 tables related to cases no. 1 to 3 and 5 to 8 in Table 4 are not presented in this paper and only useful outcomes are presented and outlined in the following sections 8.3.1 to 8.3.3, considering the effects of weight coefficient, constraint type, and objective functions, respectively.

8.3.1 Effect of weight coefficient

For item no. A in Table 5 (effect of weight coefficient), the following results are carried out:
1- For lower values of α , say $\alpha = 0.3$, the optimum values corresponded to different FML lay ups cover the predefined range for MVF variable.
2- By increasing α and number of prepreg layers (N_p), the minimum weight is reached.

8.3.2 Effect of constraints type

For item no. B in Table 5 (effect of constraint type with the response and weight objective functions), the following results are obtained:
1- The minimum impact response, as well as maximum buckling load, is occurred in case no. 4, where the constraint type is buckling only.
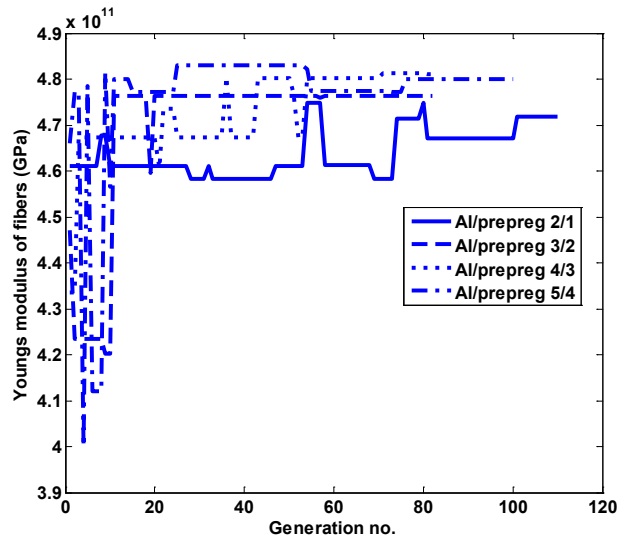
Fig. 14. Variation of E_{fi} versus *G.N.* for an Al/prepreg 2/1 FML cylindrical shell, (N_p=1).
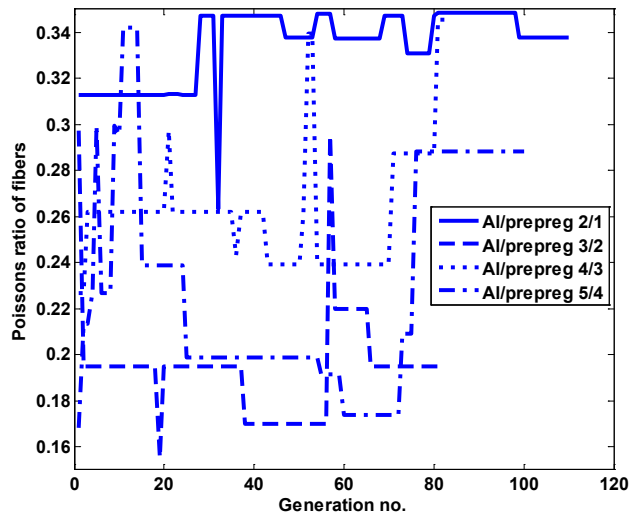

Fig. 15. Variation of ν_{fi} versus *G.N.* for an Al/prepreg 2/1 FML cylindrical shell, (N_p=1).
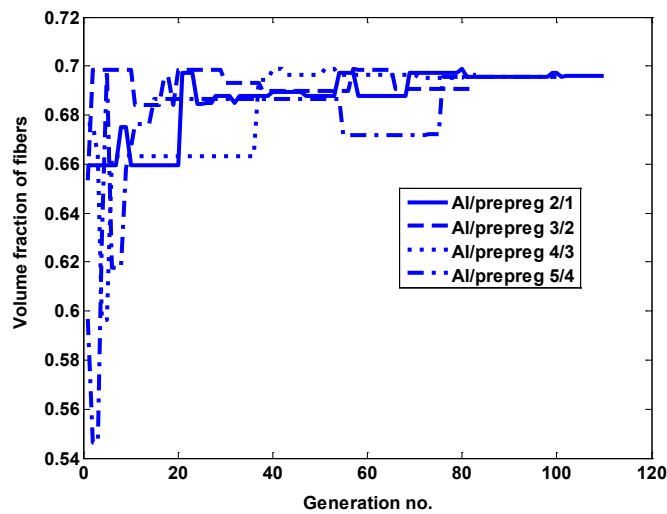

Fig. 16. Variation of V_{fi} versus *G.N.* for an Al/prepreg 2/1 FML cylindrical shell, (N_p=1).

2- The minimum weight is obtained using case no. 5, where the constraint type is strain only.

3- The effect of buckling constraint on minimum impact response as well as minimum weight is more predominant as compared to the effect of the strain constraint.

For item no. C in Table 5 (effect of constraint type with response objective function), the following results can be concluded:

1- The minimum impact response is reached in case no. 8,

where the constraint type is strain only.

2- For case no. 7, where the constraint type is buckling only, the maximum buckling load is reached. As a result, the effect of buckling constraint is more predominant in comparison with the effect of strain constraint.

8.3.3 Effect of objective functions

For item no. D in Table 5 (effect of the objective function with bucking and strain constraint), the following results are

Table 4. Classification of the optimization cases.

Objective function	Constraint type	Weight coefficient	Case no.
Response + Weight	Buckling + Strain	α=0.7	1
		α=0.5	2
		α=0.3	3
	Buckling	α=0.5	4
	Strain	α=0.5	5
Response	Buckling +Strain	α=0.5	6
	Buckling	α=0.5	7
	Strain	α=0.5	8

Table 5. Classification of the effects of optimization parameters including objective function, weight coefficient, and constraint type according to the optimization cases listed in Table 4.

Item no.	Case no. for comparison[a]	Optimization parameter for comparison
A	1 , 2 , 3	Effect of weight coefficient
B	2 , 4 , 5	Effect of constraint type
C	6 , 7 , 8	Effect of constraint type
D	2 , 6	Effect of objective function
E	4 , 7	Effect of objective function
F	5 , 8	Effect of objective function

[a] Case no. defined in Table 4.

Table 6. Results of multi-objective optimization for $\alpha = 0.5$ with buckling constraints; FML layup Al/prepreg 2/1.

Number of prepreg layers		N_p=3	N_p=2	N_p=1
Design Variables	ρ_{fi} $[\text{kg/m}^3]$	[1381/1404/1412]	[1429/1410]	[1467]
	ρ_{mi} $[\text{kg/m}^3]$	[1007/1298/1124]	[1009/1074]	[1216]
	E_{fi} [GPa]	[471/377/453]	[483/475]	[482]
	E_{mi} [GPa]	[4.64/4.93/3.63]	[4.51/5.49]	[5.48]
	ν_{fi}	[0.18/0.17/0.21]	[0.18/0.24]	[0.24]
	ν_{mi}	[0.36/0.36/0.38]	[0.30/0.34]	[0.28]
	V_{fi}	[0.65/0.52/0.68]	[0.67/0.68]	[0.70]
	MVF	0.054	0.051	0.21
	θ_i [deg]	[13.1/-39.7/-69.5]	[-26.5/-66.6]	[-71.9]
Objective Functions	w [m]	1.37e-3	1.33e-3	1.60e-3
	W [N]	342	338	360
Constraints	N_{cr} [kN/m]	1060	1210	642
	$\text{Max.}\left\{\dfrac{\varepsilon_{11}}{\varepsilon_{11}^{all}}, \dfrac{\varepsilon_{22}}{\varepsilon_{22}^{all}}, \dfrac{\gamma_{12}}{\gamma_{22}^{all}}\right\}$	1.12e-1	1.13e-1	1.87e-1

concluded:

1- For the cases where the single objective function (minimum impact response only) is desired, like case no. 2, the minimum impact response is reached.

2- The greater buckling load is corresponded to case no. 6. Since, in case no. 2, the minimum weight is one of the objective functions, a greater optimum value is obtained

for MVF.

3- As it is expected, the minimum weight could be obtained in case no. 2 where the two-objective function (including minimum weight and minimum impact response) is considered.

For item no. E in Table 5 (effect of the objective function with buckling constraint), the following results are obtained:

Table 7. Results of multi-objective optimization for $\alpha = 0.5$ with buckling constraints; FML layup Al/prepreg 3/2.

Number of prepreg layers		N_p=3	N_p=2	N_p=1
Design Variables	$\rho_{fi}\ [\text{kg/m}^3]$	[1389/1439/1387]	[1390/1432]	[1408]
	$\rho_{mi}\ [\text{kg/m}^3]$	[1061/1021/1317]	[1073/1049]	[1008]
	$E_{fi}\ [\text{GPa}]$	[455/479/482]	[478/448]	[480]
	$E_{mi}\ [\text{GPa}]$	[3.71/1.39/3.25]	[3.86/4.69]	[5.46]
	ν_{fi}	[0.15/0.20/0.23]	[0.22/0.15]	[0.24]
	ν_{mi}	[0.38/0.31/0.27]	[0.39/0.38]	[0.27]
	V_{fi}	[0.67/0.63/0.67]	[0.70/0.62]	[0.70]
	MVF	0.061	0.052	0.23
	$\theta_i\ [\text{deg}]$	[19.3/-52.9/70.65]	[55.6/12.1]	[-68.6]
Objective Functions	$w\ [\text{m}]$	1.44e-3	1.50e-3	1.58e-3
	$W\ [\text{N}]$	345	337	400
Constraints	$N_{cr}\ [\text{kN/m}]$	997	989	712
	$\text{Max.}\left\{\dfrac{\varepsilon_{11}}{\varepsilon_{11}^{all}},\dfrac{\varepsilon_{22}}{\varepsilon_{22}^{all}},\dfrac{\gamma_{12}}{\gamma_{22}^{all}}\right\}$	1.10e-1	1.69e-1	1.53e-1

Table 8. Results of multi-objective optimization for $\alpha = 0.5$ with buckling constraints; FML layup Al/prepreg 4/3.

Number of prepreg layers		N_p=3	N_p=2	N_p=1
Design Variables	$\rho_{fi}\ [\text{kg/m}^3]$	[1485/1407/1460]	[1402/1408]	[1381]
	$\rho_{mi}\ [\text{kg/m}^3]$	[1002/1162/1018]	[1053/1062]	[1266]
	$E_{fi}\ [\text{GPa}]$	[417/478/481]	[478/179]	[475]
	$E_{mi}\ [\text{GPa}]$	[2.11/5.24/5.20]	[4.03/5.50]	[5.47]
	ν_{fi}	[0.32/0.19/0.26]	[0.29/0.31]	[0.18]
	ν_{mi}	[0.32/0.32/0.36]	[0.33/0.37]	[0.26]
	V_{fi}	[0.64/0.61/0.60]	[0.64/0.65]	[0.70]
	MVF	0.055	0.060	0.213
	$\theta_i\ [\text{deg}]$	[17.5/46.0/-71.7]	[-28.4/-71.1]	[68.4]
Objective Functions	$w\ [\text{m}]$	1.51e-3	1.44e-3	1.57e-3
	$W\ [\text{N}]$	341	338	407
Constraints	$N_{cr}\ [\text{kN/m}]$	924	997	718
	$\text{Max.}\left\{\dfrac{\varepsilon_{11}}{\varepsilon_{11}^{all}},\dfrac{\varepsilon_{22}}{\varepsilon_{22}^{all}},\dfrac{\gamma_{12}}{\gamma_{22}^{all}}\right\}$	1.22e-1	1.10e-1	1.44e-1

Table 9 Results of multi objective optimization for $\alpha = 0.5$ with buckling constraints; FML layup Al/prepreg 5/4.

Number of prepreg layers		$N_p=3$	$N_p=2$	$N_p=1$
Design Variables	$\rho_{fi}\ [\text{kg/m}^3]$	[1421/1394/1557]	[1381/1384]	[1439]
	$\rho_{mi}\ [\text{kg/m}^3]$	[1005/1011/1334]	[1001/1067]	[1094]
	$E_{fi}\ [\text{GPa}]$	[437/478/479]	[473/459]	[476]
	$E_{mi}\ [\text{GPa}]$	[3.91/5.41/3.01]	[5.42/4.19]	[5.38]
	ν_{fi}	[0.16/0.19/0.31]	[0.32/0.19]	[0.26]
	ν_{mi}	[0.36/0.33/0.32]	[0.33/0.35]	[0.30]
	V_{fi}	[0.52/0.57/0.67]	[0.69/0.69]	[0.70]
	MVF	0.06	0.052	0.267
	$\theta_i\ [\text{deg}]$	[-80.6/56.2/-21.6]	[73.0/30.3]	[70.2]
Objective Functions	$w\ [\text{m}]$	1.53e-3	1.41e-3	1.56e-3
	$W\ [\text{N}]$	345	334	423
Constraints	$N_{cr}\ [\text{kN/m}]$	868	1060	742
	$\text{Max.}\left\{\dfrac{\varepsilon_{11}}{\varepsilon_{11}^{all}},\ \dfrac{\varepsilon_{22}}{\varepsilon_{22}^{all}},\ \dfrac{\gamma_{12}}{\gamma_{22}^{all}}\right\}$	1.38e-1	1.22e-1	1.51e-1

1- The minimum impact response is obtained in case no. 7, where the single objective function (minimum impact response) is considered.

2- Similar to item no. D in Table 5, the greater buckling load is corresponded to case no. 7. Since, in case no. 4, the minimum weight is one of the objective functions, a greater optimum value is obtained for MVF.

For item no. F in Table 5 (effect of the objective function with strain constraint), the following outcomes are obtained:

1- For case no. 8 (single objective function) the smaller impact response is reached.

2- Since there is no buckling constraint in cases no. 5 and 8, no special trend could be seen for weight and impact response by changing the type of objective function.

For the considered cases A to F in Table 5, the value of MVF for the case $N_p =1$ is greater than those obtained for $N_p =2$ and 3.

9. CONCLUSIONS

The impact response analysis of the FML cylindrical shells under impact load is studied and the solution is obtained using the modal technique. Multi-objective optimization of weight and impact response of FML cylindrical shells subjected to buckling and strain constraints has been investigated using GA Nine design variables (including MVF, fibre orientation, material property and volume fraction of fibre) are considered.

In the special case of Al/prepreg $[\theta/-\theta]_2$ FML cylindrical shell, the convergence of the GA is checked and the optimum values of the design variables, i.e. MVF and fibre orientations (θ) obtained by the GA are found to be very close to these found through the complete searching method.

In the following, useful outcomes of the present research are outlined:

- For a number of prepreg layers N_p greater than 1 ($N_p >1$), the smallest impact response corresponds to FML lay up 2/1 (or Al/prepreg/Al lay up).
- Irrespective of the type of FML layup, the smaller weight corresponds to a number of prepreg layers N_p greater than 1 ($N_p >1$).
- Regardless of the type of FML layup, by increasing the number of prepreg layers, after $N_p =1$, the optimum value of MVF is decreased dramatically.
- The effect of buckling constraint on minimum impact response as well as minimum weight is more predominant as compared to the effect of the strain constraint.
- As the most important result of the present study, FML layup 2/1 with a number of prepreg layers $N_p >1$ has more benefits as compared to the other layups.

The results represent a good capability of the GA to escape the local optimums and to find the global optimum rapidly. In addition, the investigations show that the considered design variables play an active role in the optimization process.

APPENDIX

$$\left[\overline{N}\right] = \begin{bmatrix} 0 & 0 & 0 & 0 & 0 \\ 0 & -\overline{N} & 0 & 0 & 0 \\ 0 & 0 & -\overline{N} & 0 & 0 \\ 0 & 0 & 0 & 0 & 0 \\ 0 & 0 & 0 & 0 & 0 \end{bmatrix}$$

$$[k_{ij}] = \begin{bmatrix} k_{11} & k_{12} & k_{13} & k_{14} & k_{15} \\ k_{21} & k_{22} & k_{23} & k_{24} & k_{25} \\ k_{31} & k_{32} & k_{33} & k_{34} & k_{35} \\ k_{41} & k_{42} & k_{43} & k_{44} & k_{45} \\ k_{51} & k_{52} & k_{53} & k_{54} & k_{55} \end{bmatrix}$$

$k_{11} = A_{11} R (\frac{\lambda}{L})^2 T_1 - \frac{A_{66}}{R} n^2 T_2$,

$k_{12} = (A_{12} + A_{66}) n T_2$, $k_{13} = A_{12} T_2$

$k_{14} = B_{11} R (\frac{\lambda}{L}) T_1 - \frac{B_{66}}{R} n^2 (\frac{L}{\lambda}) T_2$,

$k_{15} = (B_{12} + B_{66}) n T_2$

$k_{21} = -(A_{12} + A_{66})(\frac{\lambda}{L}) n T_3$,

$k_{22} = (A_{66} R + NR)(\frac{\lambda}{L}) T_3 - (\frac{A_{22}}{R} n^2 + \frac{H_{44}}{R})(\frac{L}{\lambda}) T_4$

$k_{23} = -(\frac{A_{22}}{R} + \frac{H_{44}}{R})(\frac{L}{\lambda}) n T_4$, $k_{24} = -(B_{12} + B_{66}) n T_3$

$k_{25} = (\frac{-B_{22}}{R} n^2 + H_{44})(\frac{L}{\lambda}) T_4 + B_{66} R (\frac{\lambda}{L}) T_3$

$k_{31} = -A_{12}(\frac{\lambda}{L}) T_3$, $k_{32} = -(\frac{A_{22}}{R} + \frac{H_{44}}{R})(\frac{L}{\lambda}) n T_4$

$k_{33} = (NR + H_{55} R)(\frac{\lambda}{L}) T_3 - (\frac{H_{44}}{R} n^2 + \frac{A_{22}}{R})(\frac{L}{\lambda}) T_4$,

$k_{34} = (H_{55} R - B_{12}) T_3$ $k_{35} = (H_{44} - \frac{B_{22}}{R}) n (\frac{L}{\lambda}) T_4$

$k_{41} = B_{11} R (\frac{\lambda}{L})^2 T_1 - \frac{B_{66}}{R} n^2 T_2$, $k_{42} = (B_{12} + B_{66}) n T_2$,

$k_{34} = (B_{12} - H_{55} R) T_2$

$k_{44} = D_{11}(\frac{\lambda}{L}) T_1 - (\frac{D_{66}}{R} n^2 + H_{55} R)(\frac{L}{\lambda}) T_2$,

$k_{45} = (D_{12} + D_{66}) n T_2$ $k_{51} = -(B_{12} + B_{66})(\frac{\lambda}{L}) n T_3$,

$k_{52} = (\frac{-B_{22}}{R} n^2 + H_{44})(\frac{L}{\lambda}) T_4 + B_{66} R (\frac{\lambda}{L}) T_3$

$k_{53} = (H_{44} - \frac{B_{22}}{R}) n (\frac{L}{\lambda}) T_4$, $k_{54} = -(D_{12} + D_{66}) n T_3$

$k_{55} = D_{66} R (\frac{\lambda}{L}) T_2 - (\frac{D_{22}}{R} n^2 + H_{44} R)(\frac{L}{\lambda}) T_4$

$$[M_{ij}] = \begin{bmatrix} M_{11} & 0 & 0 & M_{14} & 0 \\ 0 & M_{22} & 0 & 0 & M_{25} \\ 0 & 0 & M_{33} & 0 & 0 \\ M_{41} & 0 & 0 & M_{44} & 0 \\ 0 & M_{52} & 0 & 0 & M_{55} \end{bmatrix}$$

$M_{11} = -I_1 R T_2$, $M_{14} = -I_2 R T_2$,

$M_{12} = M_{13} = M_{15} = 0$

$M_{22} = -(I_1 + \frac{2 I_2}{R}) R (\frac{L}{\lambda}) T_4$,

$M_{25} = -(I_2 + \frac{I_3}{R}) R (\frac{L}{\lambda}) T_4$

$M_{21} = M_{23} = M_{24} = 0$

$M_{33} = -I_1 R \frac{L}{\lambda} T_4$,

$M_{31} = M_{32} = M_{34} = M_{35} = 0$

$M_{41} = -I_2 R T_2$, $M_{44} = -I_3 R (\frac{L}{\lambda}) T_2$,

$M_{42} = M_{43} = M_{45} = 0$

$M_{52} = -(I_2 + \frac{I_3}{R}) R (\frac{L}{\lambda}) T_4$, $M_{55} = -I_3 R (\frac{L}{\lambda}) T_4$,

$M_{51} = M_{53} = M_{54} = 0$

and

$T_1 = -\sin \lambda$

$T_2 = \sin \lambda$

$T_3 = (\cos \lambda - 1)$

$T_4 = -(\cos \lambda - 1)$

$\lambda = m \pi$

REFERENCES

[1] S. Khalili, R. Mittal, S.G. Kalibar, A study of the mechanical properties of steel/aluminium/GRP laminates, Materials Science and Engineering: A, 412(1-2) (2005) 137-140.

[2] A. Vlot, J.W. Gunnink, Fibre metal laminates: an introduction, Springer Science & Business Media, 2011.

[3] H. Nam, S. Jung, C. Jung, K. Han, A model of damage initiation in singly oriented ply fiber metal laminate under concentrated loads, Journal of composite materials, 37(3) (2003) 269-281.

[4] B. Geier, H.-R. Meyer-Piening, R. Zimmermann, On the influence of laminate stacking on buckling of composite cylindrical shells subjected to axial compression, Composite structures, 55(4) (2002) 467-474.

[5] T. Ng, K. Lam, J. Reddy, Dynamic stability of cylindrical panels with transverse shear effects, International Journal of solids and Structures, 36(23) (1999) 3483-3496.

[6] X. Li, Y. Chen, Transient dynamic response analysis of orthotropic circular cylindrical shell under external hydrostatic pressure, Journal of Sound and Vibration, 257(5) (2002) 967-976.

[7] K. Lam, C. Loy, Influence of boundary conditions for a thin laminated rotating cylindrical shell, Composite structures, 41(3-4) (1998) 215-228.

[8] Y.-S. Lee, K.-D. Lee, On the dynamic response of laminated circular cylindrical shells under impulse loads, Computers & structures, 63(1) (1997) 149-157.

[9] S. Matemilola, W. Stronge, Impact response of composite cylinders, International journal of solids and structures, 34(21) (1997) 2669-2684.

[10] I. Sheinman, S. Greif, Dynamic analysis of laminated shells of revolution, Journal of composite materials, 18(3) (1984) 200-215.

[11] S. Khalili, R. Azarafza, A. Davar, Transient dynamic response of initially stressed composite circular cylindrical shells under radial impulse load,

Composite Structures, 89(2) (2009) 275-284.

[12] S.W. Gong, A study of impact on composite laminated shells, National University of Singapore, 1995.

[13] R.L. Riche, R.T. Haftka, Optimization of laminate stacking sequence for buckling load maximization by genetic algorithm, AIAA journal, 31(5) (1993) 951-956.

[14] A. Smerdov, A computational study in optimum formulations of optimization problems on laminated cylindrical shells for buckling II. Shells under external pressure, Composites science and technology, 60(11) (2000) 2067-2076.

[15] P. Weaver, Design of laminated composite cylindrical shells under axial compression, Composites Part B: Engineering, 31(8) (2000) 669-679.

[16] G. Duvaut, G. Terrel, F. Léné, V. Verijenko, Optimization of fiber reinforced composites, Composite Structures, 48(1-3) (2000) 83-89.

[17] H.-T. Hu, S.-C. Ou, Maximization of the fundamental frequencies of laminated truncated conical shells with respect to fiber orientations, Composite structures, 52(3-4) (2001) 265-275.

[18] J. Park, J. Hwang, C. Lee, W. Hwang, Stacking sequence design of composite laminates for maximum strength using genetic algorithms, Composite Structures, 52(2) (2001) 217-231.

[19] S. Adali, V. Verijenko, Optimum stacking sequence design of symmetric hybrid laminates undergoing free vibrations, Composite structures, 54(2-3) (2001) 131-138.

[20] G. Soremekun, Z. Gürdal, C. Kassapoglou, D. Toni, Stacking sequence blending of multiple composite laminates using genetic algorithms, Composite structures, 56(1) (2002) 53-62.
[21] A. Jaszkiewicz, Genetic local search for multi-objective combinatorial optimization, European journal of operational research, 137(1) (2002) 50-71.

[22] R. Azarafza, S. Khalili, A. Jafari, A. Davar, Analysis and optimization of laminated composite circular cylindrical shell subjected to compressive axial and transverse transient dynamic loads, Thin-walled structures, 47(8-9) (2009) 970-983.

[23] M. Taskin, A. Arikoglu, O. Demir, Vibration and Damping Analysis of Sandwich Cylindrical Shells by the GDQM, AIAA Journal, (2019) 3040-3051.

[24] M.A. Rezvani, M. Esmaeili, M. Feizi, Discrete mass modeling for dynamic response of buildings in the vicinity of railway tracks due to train-induced ground vibrations, Scientia Iranica, 24(4) (2017) 1922-1939.

[25] A. Arikoglu, Multi-objective optimal design of hybrid viscoelastic/ composite sandwich beams by using the generalized differential quadrature method and the non-dominated sorting genetic algorithm II, Structural and Multidisciplinary Optimization, 56(4) (2017) 885-901.

[26] F. Pang, H. Li, K. Choe, D. Shi, K. Kim, Free and forced vibration analysis of airtight cylindrical vessels with doubly curved shells of revolution by using Jacobi-Ritz method, Shock and Vibration, (2017) 1-20. https://doi.org/10.1155/2017/4538540.

[27] D. Nguyen Dinh, P.D. Nguyen, The dynamic response and vibration of functionally graded carbon nanotube-reinforced composite (FG-CNTRC) truncated conical shells resting on elastic foundations, Materials, 10(10) (2017) 1194.

[28] M. Talebitooti, M. Ghasemi, S. Hosseini, Vibration analysis of functionally graded cylindrical shells with different boundary conditions subjected to thermal loads, Journal of Computational & Applied Research in Mechanical Engineering (JCARME), 6(2) (2017) 103-114.

[29] J.R. Vinson, The behavior of shells composed of isotropic and composite materials, Springer Science & Business Media, 2013.

[30] A. Jafari, S. Khalili, R. Azarafza, Transient dynamic response of composite circular cylindrical shells under radial impulse load and axial compressive loads, Thin-Walled Structures, 43(11) (2005) 1763-1786.

[31] S. Tsai, Introduction to composite materials, Routledge, 2018.

[32] R. Olsson, Mass criterion for wave controlled impact response of composite plates, Composites Part A: Applied Science and Manufacturing, 31(8) (2000) 879-887.

[33] K. Shivakumar, W. Elber, W. Illg, Prediction of impact force and duration due to low-velocity impact on circular composite laminates, 23(3) (1985) 442-449.

[34] S.R. Swanson, Limits of quasi-static solutions in impact of composite structures, Composites Engineering, 2(4) (1992) 261-267.

[35] S. Abrate, Impact on composite structures, Cambridge university press, 2005.

[36] G.A. Soremekun, Genetic algorithms for composite laminate design and optimization, Virginia Tech, 1997.

[37] H. Altenbach, J. Altenbach, W. Kissing, Mechanics of composite structural elements, Springer, 2018.

[38] D.E. Hodgson, M.H. Wu, R.J. Biermann, ASM Handbook, Volume 2, Properties and Selection, Nonferrous Alloys and Special-Purpose Materials, in, ASM Handbook Committee (Materials Park: ASM International), 1990.